17. Davidson, E. A. & Trumbore, S. E. Gas diffusivity and production of CO_2 in deep soils of the eastern Amazon. *Tellus B* **47,** 550–565 (1995).
18. Richey, J. E., Victoria, R. L., Mayorga, E., Martinelli, L. A. & Meade, R. H. in *Biospheric Feedbacks in Climate and the Hydrological Cycle* (ed. Kabat, P.) (Springer, in the press).
19. McClain, M. E., Richey, J. E., Brandes, J. A. & Pimentel, T. P. Dissolved organic matter and terrestrial-lotic linkages in the central Amazon Basin, Brazil. *Glob. Biogeochem. Cycles* **11,** 295–311 (1997).
20. Melack, J. M. & Forsberg, B. R. in *The Biogeochemistry of the Amazon Basin* (eds McClain, M. E., Victoria, R. L. & Richey, J. E.) 235–274 (Oxford Univ. Press, New York, 2001).
21. Chambers, J. Q., dos Santons, J., Ribeiro, R. J. & Higuichi, N. Tree damage, allometric relationships, and above-ground net primary production in central Amazon forest. *Forest Ecol. Management* **5348,** 1–12 (2000).
22. Devol, A. H., Forsberg, B. R., Richey, J. E. & Pimentel, T. P. Seasonal variation in chemical distributions in the Amazon (Solimões) River: a multiyear time series. *Glob. Biogeochem. Cycles* **9,** 307–328 (1995).
23. Siqueira, P. *et al.* A continental-scale mosaic of the Amazon Basin using JERS-1 SAR. *IEEE Trans. Geosci. Remote Sensing* **38,** 2638–2644 (2000).
24. Barbosa, C., Hess, L., Melack, J. & Novo, E. Mapping Amazon Basin wetlands through region-growing segmentation and segmented-based classification of JERS-1 data. *IX Latin Am. Symp. Remote Sensing (6–10 November 2000)* 1168–1176 (Universidad Nacional de Lujan, Puerto Iguazu, Argentina, 2000); see also ⟨http://www.selper.org⟩.
25. Hess, L. L. *et al.* Geocoded digital videography for validation of land cover mapping in the Amazon Basin. *Int. J. Remote Sensing* (in the press).
26. Sippel, S. J., Hamilton, S. K., Melack, J. M. & Novo, E. M. Passive microwave observations of inundation area and the area/stage relation in the Amazon River floodplain. *Int. J. Remote Sensing* **19,** 3055–3074 (1998).
27. Richey, J. E., Devol, A. H., Wofsy, S. C., Victoria, R. & Ribeiro, M. N. G. Biogenic gases and the oxidation and reduction of carbon in the Amazon River and floodplain waters. *Limnol. Oceanogr.* **33,** 551–561 (1988).
28. Devol, A. H., Quay, P. D., Richey, J. E. & Martinelli, L. A. The role of gas exchange in the inorganic carbon, oxygen and 222 radon budgets of the Amazon River. *Limnol. Oceanogr.* **32,** 235–248 (1987).
29. Clark, J. F., Wanninkhof, R., Schlosser, P. & Simpson, H. J. Gas exchange rates in the tidal Hudson River using a dual tracer technique. *Tellus B* **46,** 264–285 (1994).
30. MacIntyre, S., Eugster, W. & Kling, G. W. in *Gas Transfer at Water Surfaces* (eds Donelan, M. A., Drennan, W. M., Saltzman, E. S. & Wanninkhof, R.) 135–139 (American Geophysical Union, Washington, 2001).

Acknowledgements

We thank E. Mayorga, S. Denning, M. Gastil, D. Montgomery, R. Victoria, A. Krusche, A. Devol, P. Quay and J. Hedges for technical assistance and discussions, B. Forsberg and T. Pimental for fieldwork, and the Global Rain Forest Mapping Project of the National Space Development Agency of Japan for providing the JERS-1 radar data. This work was supported by the US NSF and NASA EOS and LBA projects, and by the Brazilian FAPESP programme.

Competing interests statement

The authors declare that they have no competing financial interests.

Correspondence and requests for materials should be addressed to J.E.R. (e-mail: jrichey@u.washington.edu).

Small-scale structure of the geodynamo inferred from Oersted and Magsat satellite data

Gauthier Hulot*, Céline Eymin*, Benoît Langlais*, Mioara Mandea* & Nils Olsen†

** Département de Géomagnétisme et Paléomagnétisme, CNRS UMR 7577, Institut de Physique du Globe de Paris, 4 Place Jussieu, B89, Tour 24, 75252 Paris cedex 05, France*
† Center for Planetary Science, Danish Space Research Institute, Julianes Maries Vej 30, DK-2100 Copenhagen, Denmark

The 'geodynamo' in the Earth's liquid outer core produces a magnetic field that dominates the large and medium length scales of the magnetic field observed at the Earth's surface[1,2]. Here we use data from the currently operating Danish Oersted[3] satellite, and from the US Magsat[2] satellite that operated in 1979/80, to identify and interpret variations in the magnetic field over the past 20 years, down to length scales previously inaccessible. Projected down to the surface of the Earth's core, we found these variations to be small below the Pacific Ocean, and large at polar latitudes and in a region centred below southern Africa. The flow pattern at the surface of the core that we calculate to account for these changes is characterized by a westward flow concentrated in retrograde polar vortices and an asymmetric ring where prograde vortices are correlated with highs (and retrograde vortices with lows) in the historical (400-year average) magnetic field[4,5]. This pattern is analogous to those seen in a large class of numerical dynamo simulations[6], except for its longitudinal asymmetry. If this asymmetric state was reached often in the past, it might account for several persistent patterns observed in the palaeomagnetic field[7–10]. We postulate that it might also be a state in which the geodynamo operates before reversing.

Thanks to the recent launch of the Danish Oersted satellite[3] (inclination 96.5°, altitude 638–849 km), 20 years after the 1979/80 US Magsat[2] analogous mission (97°, 325–550 km), two data sets at two different epochs are now available that can be used to construct high-degree spherical harmonic models of the geomagnetic field. (Degree 1 is the dipole field; the larger the degree, the smaller the length scale.) Taking advantage of this opportunity and relying on models[11] well suited for that purpose, we compute and investigate the changes that have occurred in the geomagnetic field between 1980 and 2000, focusing on the large to medium scales (that is, up to

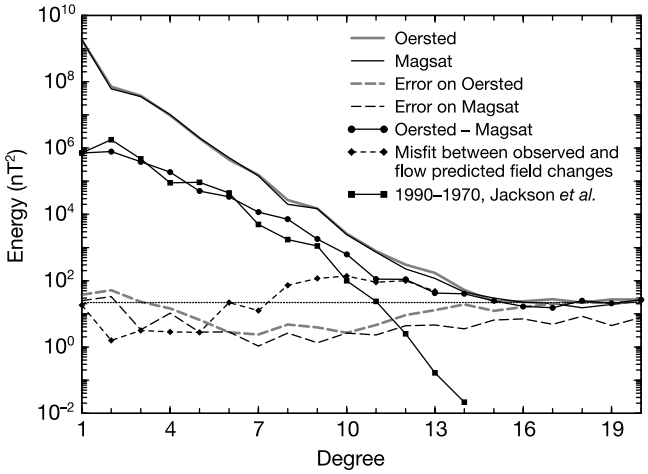

Figure 1 Spectra of the Oersted and Magsat models[11], of their error, of their difference, and of how well flows predict this difference. The spectrum of a model is constructed by plotting the contribution of each degree n of the spherical harmonic expansion to the average $\langle \mathbf{B}^2 \rangle$ of the predicted field **B** over the Earth's surface[1,2]. Errors in the Oersted and Magsat models are computed by analysing differences between models based on various data subsets[11]. Note the well-known[2] knee within the Oersted and Magsat spectra, showing that the main field probably dominates the signal for degrees less than 13, whereas the crustal field dominates for degrees larger than 15. A similar knee is seen around degree 15, in the Oersted–Magsat spectrum of the difference between the Oersted and Magsat fields. This knee, and the flat section of the spectrum beyond it, reveals disagreements between the high-degree signal sensed by Oersted and Magsat at a level slightly less than that of the crustal signal itself[12]. Up to degree 13, however, the Oersted–Magsat spectrum is well above the level (dotted line) defined by both that flat section and the crustal spectrum (the contribution of which is believed to be weaker at low degrees than at high degrees[2]). It is also well above the error level. It thus cannot be attributed to noise or a crustal source. By contrast, it can be explained by core surface flows, as is illustrated by the spectrum of the misfit between the predicted and the observed Oersted minus Magsat field difference. This misfit is at a level comparable to that of the errors in the models and of crustal contributions, but relaxed at the largest degrees to account for 'truncation errors'[17]. For reference, the spectrum of the less-resolved field variations[5] between 1970 and 1990 is also shown.

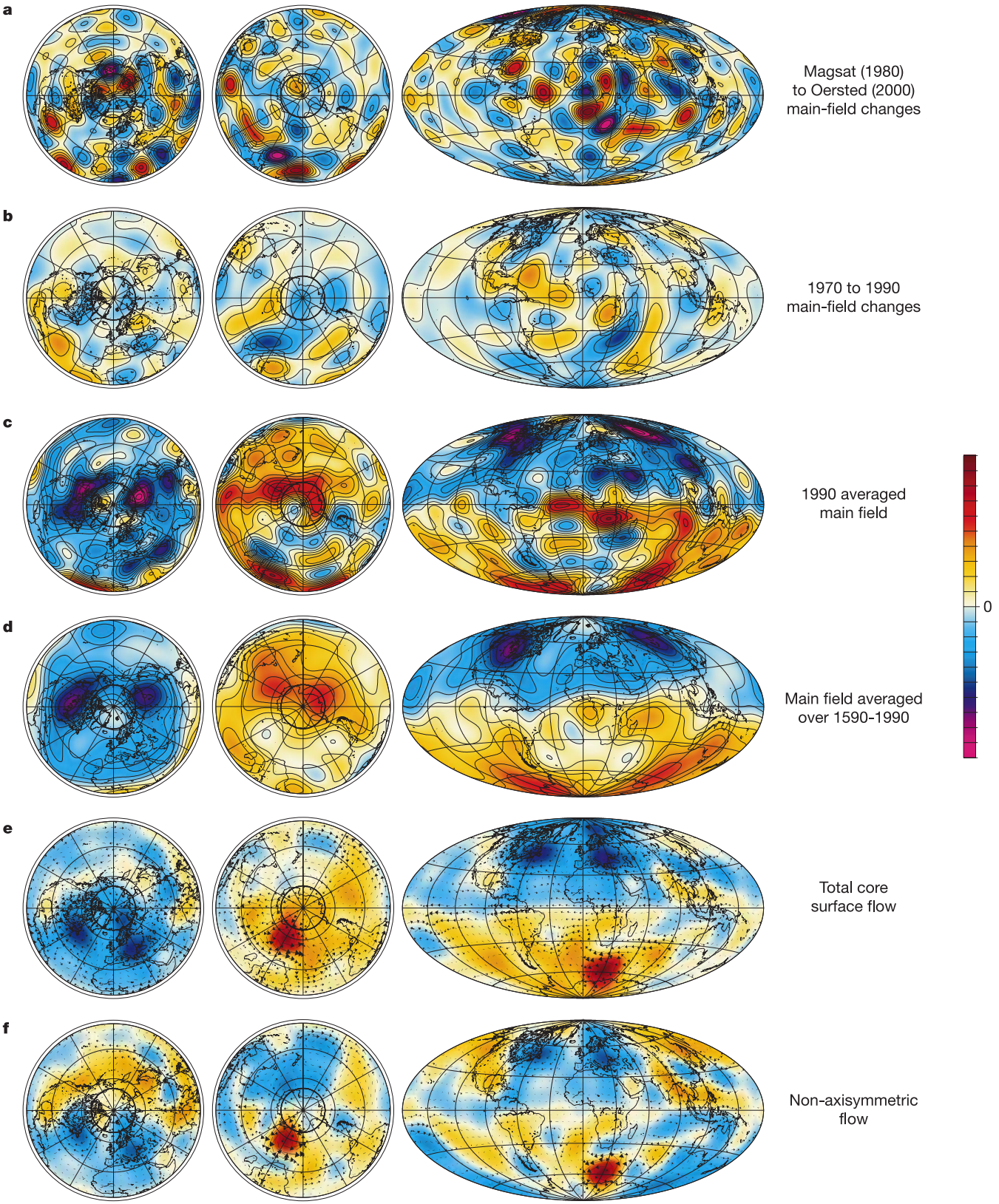

Figure 2 Polar (north and south) and Hammer views of the small-scale structure of the geodynamo at the core surface. **a**, Changes in the radial component of the field between 1980 (Magsat) and 2000 (Oersted) (− 340 μT to 333 μT). **b**, Analogous but less-resolved field changes between 1970 and 1990 (computed from the historical model of ref. 5, −186 μT to 147 μT). **c**, The radial component of the average 1990 main field computed by averaging the Magsat and Oersted main-field models[11] (−1,032μT to 908μT). **d**, The main field averaged over the historical period 1590–1990 (computed from the model of ref. 5, -745 μT to 594 μT). **e**, Core surface flow accounting for the main-field changes in **a** by advecting the 1990 main field in **c** (arrows for the flow, maximum of 50 km yr^{-1}, colour code for the toroidal scalar associated to the flow). **f**, Same as in **e** but for the non-axisymmetric component of the flow (maximum 65 km yr^{-1}). In all figures, there is a linear colour code: red positive, blue negative, renormalized to the maximum absolute value, except for **b** (respectively **d**) which uses the same scale as **a** (respectively **c**). Contours every 50 μT in **a** and **b**, every 100 μT in **c** and **d**. Also shown in each polar plot, the surface trace of the tangent cylinder.

degree 13) thought to be dominated by the main field produced by the geodynamo[1,2] (Fig. 1).

Figure 2a shows the radial component of those changes plotted at the core surface where the main field originates. Most remarkable are the large changes, which occurred at high, especially northern, latitudes, and in a hemispheric region centred below Africa. These regions contrast strongly with a wide region below the Pacific, where far fewer changes occurred. This pattern could not be resolved as clearly before the Oersted mission (ref. 5, Fig. 2b), and is robust against model uncertainties (Fig. 1).

We now consider if this pattern could have been produced by sources other than the geodynamo—perhaps in the crust, ionosphere or magnetosphere. Although formal separation of the signals from these sources is only possible in part, over many years a framework for practical separation has been constructed[2], and the results of such separation suggest that this could hardly be the case. First, we consider crustal signals. These are thought to dominate the field at degree 15 and above (Fig. 1). But there is no evidence at these wavelengths for any large changes in the field between 1980 and 2000[12], and at longer wavelengths, even a 100% change in the estimated crustal signal would produce weak field changes (Fig. 1). Second, ionospheric signals. In the field models on which we rely[11], these signals have been carefully minimized by using night-side measurements on magnetically quiet days, and field-aligned currents at high latitudes have specifically been removed by using only field intensity data there. The remaining ionospheric contamination at the Earth's surface can then be estimated to be less than 10 nT at all latitudes in the Magsat (1980) model[2], and probably less in the Oersted (2000) model. Much of this field would in addition show up in zonal fields in Fig. 2a, as the data for each model were recorded at similar local times. Such characteristics do not match the typical 100-nT change (mainly in the degrees 8 to 13 and dominantly not in zonal fields) implied at the Earth's surface by the intense small-scale structures seen in Fig. 2a. Magnetospheric signals can also easily be dismissed, as they are large-scale and can be formally separated from the core signal[2]. Finally, signals from electrical currents induced in the crust and upper mantle by all those external sources can again be shown to be too weak[13,14]. Therefore, the results in Fig. 2a are most likely to be due to the temporal (secular) variation of the main field.

This secular variation is the combined consequence of main-field diffusion through ohmic dissipation and main-field advection by flows at the core surface[15]. Previous studies[16,17] have shown that much of the short-term large-scale variations of the main field could be explained in terms of its advection by surface flows satisfying the tangentially geostrophic balance[18] (which assumes that the horizontal component of the Coriolis forces is mainly balanced by a dynamical pressure gradient), in the so-called 'frozen-flux approximation'[15] (which assumes diffusion to be negligible). Core flows inferred in this way have further been shown to account for length of day variations on decade timescales (by angular momentum exchange with the mantle)[19–21], and to reflect dynamical features, akin to torsional oscillations predicted by dynamo theory[22,21]. We thus decided to try and compute a tangentially geostrophic flow, which would account for the observed main-field changes (Fig. 2a).

To do this, we computed the average of the two 1980 and 2000 main-field models (Fig. 2c), together with the average secular variation accounting for the 1980 to 2000 main-field changes. We finally computed the flow producing this average secular variation by advection of the average main-field model. We relied on the numerical procedure of ref. 21 with some adjustments. More details about this computation will be provided elsewhere (C.E. and G.H., manuscript in preparation). Most important here is the fact that the flow that we computed (Fig. 2e) succeeds at predicting the field changes at a satisfactory level (see Fig. 1).

Figure 2e reveals a flow with a number of strong vortices embedded in a mainly westward axisymmetric flow. This axisymmetric flow (detailed in Fig. 3) is remarkably symmetric with respect to the equator. It consists mainly of a westward body rotation of the core with respect to the mantle (of order $0.1^\circ\,yr^{-1}$) and two strong westward ('retrograde' when compared to the Earth's daily rotation) polar vortices (of order $0.9^\circ\,yr^{-1}$, the northern vortex being slightly larger) within the 'tangent cylinder' (tangent to the inner core and intersecting the core surface at latitude $\pm 69.5^\circ$). The body rotation is a well-known feature. It varies with time as a result of core–mantle coupling acting on decade timescales[16,19–21]. Far less is known about the polar vortices, which confine most of the westward drift at high latitude and appear to be important in explaining the changes seen near both poles in Fig. 2a. Recently, similar vortices have been tentatively found with the help of computations based on less-resolved historical models[21,23]. These vortices may thus have been active over at least the past century, and could be permanent features of the geodynamo. Figure 3 also shows a small-scale zonal flow that we believe is the result of a Gibbs effect produced by the flow computation, which still fails to resolve the finest details of the probably sharp boundaries of the polar vortices[21]. We finally note that no significant medium-scale zonal flow is present in Fig. 3. This suggests that the torsional oscillations are currently of low amplitude, a result consistent with both the general trend seen in core flows computed over the past century[21] and the relatively short decay time which has been inferred for those oscillations[22].

Plotting the non-axisymmetric flow alone leads to another interesting result (Fig. 2f). This part of the flow displays a medium- to high-latitude ring of vortices roughly, but not exactly, symmetrical with respect to the equator, and clustering around the tangent cylinder. This is best seen by also plotting the toroidal scalar associated with the flow, which can be viewed as a filtered (low-pass) measure of the radial vorticity $\omega_r = \mathbf{n}\cdot(\nabla \times \mathbf{u})$ of the flow $\mathbf{u}$. The colour code in Fig. 2e and f is then such that prograde and retrograde vortices appear respectively red and blue in the Northern Hemisphere, and respectively blue and red in the Southern Hemisphere (note that equatorial-symmetric flows translate into anti-symmetric radial vorticity). Computations based on historical models could not resolve these vortices as clearly[16,17]. They are reminiscent of analogous vortices seen in many numerical simulations of the geodynamo[6,24,25]. The class of simulations that are referred to in ref. 6 as being in a 'fully developed regime' (see also ref. 24) also display retrograde polar vortices analogous to those

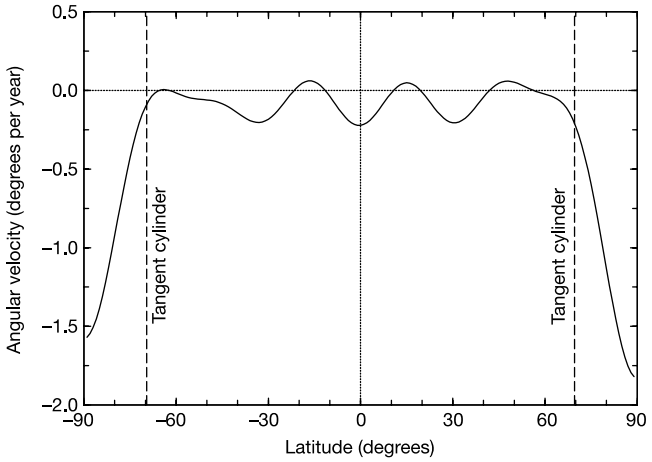

Figure 3 Axisymmetric component of the flow at the core surface. This azimuthal flow is plotted in terms of angular velocity about the Earth's rotation axis (positive for eastward with respect to the mantle, negative for westward) as a function of latitude. Note the general westward trend, and the strong westward flows at high latitudes. These flows correspond to retrograde polar vortices occurring within the tangent cylinder (beyond $\pm 69.5^\circ$ of latitude); see text.

identified in Fig. 3. Also, for such dynamos, computing surface flows as we did has been shown to lead to a reasonable surface picture of the full dynamo flows, provided those flows are not too small scale[26]. Even though it is known that such numerical simulations are still forced to use unrealistic dimensionless numbers[27], this suggests that the geodynamo could belong to a similar 'class' of dynamos.

For such dynamos, it has also been observed that prograde vortices are associated with slow downwelling flows, which concentrate the flux inside the vortices on the long term. By contrast, retrograde vortices are associated with slow upwelling flows, which tend to expel field of reversed polarity (compared to that of the main dipole field) from within the core. It has been speculated that a similar phenomenon could take place in the Earth's core[28]. In Fig. 2f, prograde vortices (red in the North, blue in the South) tend to occur in a region where maxima are seen in the main field (where the so-called 'flux bundles'[4,28] are found, Fig 2c). By contrast, retrograde vortices (blue in the North, red in the South) occur where the main field tends to be minimum, if not of reversed polarity. This correlation is much clearer when made with the main field averaged over the past 400 years (Fig. 2d). Analogous up- and downwelling flows (weak and non-geostrophic, hence not directly visible in Fig. 2f which shows the first-order flow computed under the tangentially geostrophic assumption) could thus be responsible for the global structure of the main field averaged over secular timescales.

One characteristic of the geodynamo remains puzzling: its azimuthal asymmetry. In most numerical dynamos, prograde and retrograde vortices tend to alternate around the tangent cylinder. In Fig. 2f, the flow in the 'Pacific hemisphere' is mainly made up of prograde vortices, contrasting with the flow in the other hemisphere where strong retrograde vortices are found. This is also where the strongest field changes are seen at present (Fig. 2a), and where most of the reversed polarity field has been produced in the past 400 years (which led to the creation of the large reverse patch now seen below South Africa in Fig. 2c)[4]. Archaeomagnetic data further suggest that significant changes have occurred in the (large-scale) main field over the past 3,000 years (ref. 29), and that the present main-field pattern is a relatively recent feature. This leads us to speculate that in the past millennium, retrograde vortices could have progressively vanished in the Pacific hemisphere, while gaining momentum and increasing the rate of creation of reversed polarity field in the other hemisphere. At the present time, the changes that this would have produced in the main field would still be affected by the strong main flow associated with the vortices, leading to the locally enhanced field changes seen in Fig. 2a. It could thus be that the asymmetry at present observed in all maps of Fig. 2 is only temporary. This would be consistent with the results of the only dynamo explicitly displaying a similar azimuthal asymmetry, which is indeed only temporarily observed[25].

Palaeomagnetic data can then be used to try and gain further insight into this question. The present asymmetric main field is also associated with a significantly enhanced order 1 (that is, $\cos\phi$) non dipole field component[1,7]. If this were to happen often enough, it could explain most of the behaviour of the palaeosecular variation over the past 5 Myr (refs 1, 7). This then further suggests that, although possibly temporary, the present asymmetric state of the geodynamo could be frequently reached. If this state were preferentially reached in a fixed way with respect to the mantle, as a result of its likely influence on the core, it could also eventually produce an averaged palaeomagnetic field showing traces of 'flux bundles'[4,28] as in Fig. 2d. But whether such traces can in fact be seen in the palaeomagnetic field remains an open question[8,30].

The growth of the South African patch could also be associated with the present rapid decrease of the dipole field—a decrease that some[9,10] have suggested could eventually lead to a reversal sharing characteristics with the last known reversal (780 kyr ago[1]). Although this does not prove that a new reversal is impending, it suggests that the asymmetric state we are witnessing at present is one through which the geodynamo could also possibly go just before reversing. □

Received 4 December 2001; accepted 4 February 2002.

1. Merrill, R. T., McElhinny, M. W. & McFadden, P. L. *The Magnetic Field of the Earth, Paleomagnetism, the Core and the Deep Mantle* (Academic, San Diego, 1996).
2. Langel, R. A. & Hinze, W. J. *The Magnetic Field of the Earth's Lithosphere, The Satellite Perspective* (Cambridge Univ. Press, Cambridge, 1998).
3. Neubert, T. *et al.* Oersted satellite captures high-precision geomagnetic field data. *Eos* **82,** 81, 87–88 (2001).
4. Bloxham, J., Gubbins, D. & Jackson, A. Geomagnetic secular variation. *Phil. Trans. R. Soc. Lond. A* **329,** 415–502 (1989).
5. Jackson, A., Jonkers, A. R. T. & Walker, M. R. Four centuries of geomagnetic secular variation from historical records. *Phil. Trans. R. Soc. Lond. A* **358,** 957–990 (2000).
6. Olson, P., Christensen U. & Glatzmaier, G. Numerical modeling of the geodynamo: Mechanisms of field generation and equilibration. *J. Geophys. Res.* **104,** 10383–10404 (1999).
7. Hulot, G. & Gallet, Y. On the interpretation of virtual geomagnetic pole (VGP) scatter curves. *Phys. Earth. Planet. Inter.* **95,** 37–53 (1996).
8. Gubbins, D. & Kelly, P. Persistent pattern in the geomagnetic field over the past 2.5 Myr. *Nature* **365,** 829–832 (1993).
9. Gubbins, D. & Coe, R. Longitudinally confined geomagnetic reversal paths from non-dipole transition fields. *Nature* **362,** 51–53 (1993).
10. Constable, C. Link between geomagnetic reversal paths and secular variation of the field over the past 5 Myr. *Nature* **358,** 230–233 (1992).
11. Langlais, B., Mandea, M. & Ultré-Guérard, P. High-resolution magnetic field modelling: application to MAGSAT and Oersted data. *Phys. Earth. Planet. Inter.* (in the press).
12. Purucker, M., Langlais, B., Olsen, N., Hulot, G. & Mandea, M. The southern edge of cratonic North America: Evidence from new satellite magnetometer observations. *Geophys. Res. Lett.* (in the press).
13. Olsen, N. Induction studies with satellite data. *Surv. Geophys.* **20,** 309–340 (1999).
14. Tarits, P. & Naphsica, G. Electromagnetic induction effects by the solar quiet magnetic field at satellite altitude. *Geophys. Res. Lett.* **27,** 4009–4012 (2000).
15. Roberts, P. H. & Scott, S. On the analysis of the secular variation. 1. A hydromagnetic constraint: Theory. *J. Geomagn. Geoelectr.* **17,** 137–151 (1965).
16. Bloxham, J. & Jackson, A. Fluid flow near the surface of Earth's outer core. *Rev. Geophys.* **29,** 97–120 (1991).
17. Hulot, G., Le Mouël, J. L. & Wahr, J. Taking into account truncation problems and geomagnetic model accuracy in assessing computed flows at the core-mantle boundary. *Geophys. J. Int.* **108,** 224–246 (1992).
18. Le Mouël, J. L. Outer core geostrophic flow and secular variation of Earth's magnetic field. *Nature* **311,** 734–735 (1984).
19. Jault, D., Gire, C. & Le Mouël, J. L. Westward drift, core motions and exchanges of angular momentum between core and mantle. *Nature* **333,** 353–356 (1988).
20. Jackson, A., Bloxham, J. & Gubbins, D. in *Dynamics of Earth's Deep Interior and Earth Rotation* (eds Le Mouël, J.-L. *et al.*) 97–107 (IUGG Vol. 12, AGU Geophysical Monograph 72, American Geophysical Union, Washington DC, 1993).
21. Pais, A. & Hulot, G. Length of day decade variations, torsional oscillations and inner core superrotation: evidence from recovered core surface zonal flows. *Phys. Earth. Planet. Inter.* **118,** 291–316 (2000).
22. Zatman, S. & Bloxham, J. Torsional oscillations and the magnetic field within the Earth's core. *Nature* **388,** 760–763 (1997).
23. Olson, P. & Aurnou, J. A polar vortex in the Earth's core. *Nature* **402,** 170–173 (1999).
24. Glatzmaier, G. & Roberts, P. A three-dimensional convective dynamo solution with rotating and finitely conducting inner core and mantle. *Phys. Earth. Planet. Inter.* **91,** 63–75 (1995).
25. Kuang, W. & Bloxham, J. in *The Core-Mantle Boundary Region* (eds Gurnis, M. *et al.*) 187–208 (Geodyn. Ser. 28, American Geophysical Union, Washington DC, 1998).
26. Rau, S., Christensen, U., Jackson, A. & Wicht, J. Core flow inversion tested with numerical dynamo models. *Geophys. J. Int.* **141,** 485–497 (2000).
27. Dormy, E., Valet, J. P. & Courtillot, V. Numerical models of the geodynamo and observational constraints. *Geochem. Geophys. Geosyst.* **1,** 62 (2000).
28. Gubbins, D. & Bloxham, J. Morphology of the geomagnetic field and implications for the geodynamo. *Nature* **325,** 509–511 (1987).
29. Constable, C. G., Johnson, C. L. & Lund, S. P. Global geomagnetic field models for the past 3000 years: transient or permanent flux lobes?*Phil. Trans. R. Soc. Lond. A* **358,** 991–1008 (2000).
30. Carlut, J. & Courtillot, V. How complex is the Earth's average magnetic field?*Geophys. J. Int.* **134,** 527–544 (1998).

Acknowledgements

We thank those involved in the Oersted project for their contribution to this work. The Oersted project is funded by the Danish Ministry of Transport, the Ministry of Research and Information Technology, and the Ministry of Trade and Industry of Denmark. Additional support for Oersted came from NASA, the Centre National d'Etudes Spatiales (CNES) and DARA. We also thank R. Holme for comments and suggestions.

Competing interests statement

The authors declare that they have no competing financial interests.

Correspondence and requests for materials should be addressed to G.H. (e-mail: gh@ipgp.jussieu.fr).